Neurobiology of Disease 33 (2009) 459–466

Contents lists available at ScienceDirect

Neurobiology of Disease

journal homepage: www.elsevier.com/locate/ynbdi

Minocycline restores striatal tyrosine hydroxylase in GDNF heterozygous mice but not in methamphetamine-treated mice

Heather A. Boger [a], Lawrence D. Middaugh [a,b], Ann-Charlotte Granholm [a], Jacqueline F. McGinty [a,b,*]

[a] Department of Neurosciences and Center on Aging, Medical University of South Carolina 173 Ashley Avenue BSB 403, Charleston, SC 29425, USA
[b] Department of Psychiatry, Medical University of South Carolina, Charleston, SC 29425, USA

ARTICLE INFO

Article history:
Received 30 July 2008
Revised 12 November 2008
Accepted 27 November 2008
Available online 9 December 2008

Keywords:
Dopamine
Striatum
Substantia nigra
Neuroinflammation
Neurotoxicity
Neurotrophins
Transgenic mice

ABSTRACT

Inflammation, phospho-p38 MAPK activation, and a reduction in glial cell line-derived neurotrophic factor (GDNF) occur in Parkinson's disease. Microglial activation in the substantia nigra and a tyrosine hydroxylase deficit in the striatum of 3-month-old GDNF heterozygous ($GDNF^{+/-}$) mice were previously reported and both were exacerbated by a toxic methamphetamine binge. The current study assessed the effects of minocycline on these methamphetamine-induced effects. Minocycline (45 mg/kg, i.p.×14 days post-methamphetamine or saline injections) reduced microglial activation and phospho-p38 MAPK in the substantia nigra of saline-treated $GDNF^{+/-}$ mice and in methamphetamine-treated wildtype and $GDNF^{+/-}$ mice. Although minocycline increased tyrosine hydroxylase-immunoreactivity in $GDNF^{+/-}$ mice, it did not attenuate the methamphetamine-induced reduction of tyrosine hydroxylase. The results suggest that neuroinflammation is deleterious to the dopamine system of $GDNF^{+/-}$ mice but is not the primary cause of methamphetamine-induced damage to the dopamine system in either $GDNF^{+/-}$ or wildtype mice.

Introduction

Mice with a partial deletion of glial cell line-derived neurotrophic factor (GDNF) are more vulnerable than wildtype (WT) mice to the neurotoxic effects of the dopaminergic (DAergic) neurotoxin, methamphetamine (METH) (Boger et al., 2007). Possible anti-inflammatory properties of GDNF are suggested by greater microglia activation in the substantia nigra (SN) of 3-month-old $GDNF^{+/-}$ compared to age-matched WT mice. METH exacerbated microgliosis in the SN and tyrosine hydroxylase (TH) depletion in the striatum of $GDNF^{+/-}$ mice; however, the mechanisms are unknown.

High METH doses produce a swift and transient increase in reactive astrogliosis (Sheng et al., 1994; Hebert and O'Callaghan, 2000) and microgliosis in the striatum (Lavoie et al., 2004; Thomas et al., 2004a, b). Striatal microgliosis was resolved within 1 week in the latter study and within 2 weeks in our recent study (Boger et al., 2007). Microgliosis in SN was absent 2 days after the METH binge in the study of Thomas et al. (2004b); however, it was present 2 weeks after the METH binge in our study, suggesting a delayed microgliotic response without a simultaneous DA cell body loss. In addition to glial activation, METH induces protein phosphorylation cascades that are associated with inflammation and cellular stress (Hebert and O'Callaghan, 2000). Cellular stressors activate the p38 MAPK pathway which has been implicated in neuronal cell death associated with axotomy and excitotoxicity (Glicksman et al., 1998; Kawasaki et al., 1997). Further, p38 MAPK mediates pro-inflammatory cytokine production in a variety of cell types (Lee et al., 1994; Chen and Wang, 1999; Hendricks et al., 2008), including microglia (Bhat et al., 1998). Inhibition of p38 MAPK activation improves DA neuronal survival both in culture and after neurotransplantation in a rat model of Parkinson's disease (PD; Zawada et al., 2001). However, to date induction of the p38 MAPK pathway by METH has not been reported.

Minocycline, a tetracycline-related antibiotic, has anti-inflammatory (Tikka and Koistinaho, 2001; Tikka et al., 2001) and anti-apoptotic properties (Zhu et al., 2002; Wang et al., 2004). Minocycline easily crosses the blood–brain barrier and is reported to reduce neurodegeneration in animal models of ischemia (Yrjanheikki et al., 1998, 1999), amyotrophic lateral sclerosis (ALS; Zhu et al., 2002; Kriz et al., 2002), Huntington's disease (HD; Chen et al., 2000; Wang et al., 2003), and PD (Du et al., 2001; Wu et al., 2002; Quintero et al., 2006). The treatment potential for minocycline, however, is tempered by additional reports that it can exacerbate brain injury in animal models of PD, HD, and ischemia (Diguet et al., 2004; Yang et al., 2003; Tsuji et al., 2004; Sriram et al., 2006), as well as ALS symptoms in a clinical trial (Gordon et al., 2007). Despite the controversy over its positive vs. negative effects, the efficacy and safety of minocycline are being evaluated in clinical trials for PD and HD (Blum et al., 2004; LeWitt and Taylor 2008).

In the present study, we used a minocycline treatment regimen, demonstrated to be neuroprotective in two different models of

* Corresponding author. Fax: +1 843 792 4423.
E-mail address: mcginty@musc.edu (J.F. McGinty).
Available online on ScienceDirect (www.sciencedirect.com).

0969-9961/$ – see front matter © 2008 Elsevier Inc. All rights reserved.
doi:10.1016/j.nbd.2008.11.013

neurotoxicity in our laboratories (Hunter et al., 2004; Quintero et al., 2006), to investigate whether suppression of inflammation would attenuate METH-induced DAergic damage in the striatum of GDNF$^{+/-}$ vs. WT mice.

Materials and methods

Experimental design

Young adult GDNF$^{+/-}$ and WT mice, 2.5 months of age, were injected 4 times at 2 h intervals with methamphetamine hydrochloride (10 mg/kg, i.p., Sigma-Aldrich) or saline (0.2 ml 0.9% NaCl, i.p.) as outlined in Fig. 1. Rectal temperatures were recorded 20 min prior to the 1st injection and 20 min after each METH injection and motor activity was recorded after the first and fourth injections as previously reported (Boger et al., 2007). Starting 24 h after the last METH injection, mice from the two genotypes were injected for 14 days with minocycline hydrochloride (45 mg/kg, i.p. MP Biomedicals) or saline (0.2 ml 0.9% NaCl, i.p.). The final experimental design was a 2 (Genotype)×2 (METH Binge)×2 (Minocycline Treatment) factorial with N=8 in each group. After the 14-day minocycline regimen, motor activity was assessed before the mice were perfusion-fixed and brains sectioned for immunohistochemical detection of TH, CD45 (marker of microglia activation), and phospho-p38 MAPK.

Animals

GDNF$^{+/-}$ mice were compared to their WT littermates in all experiments. The nonfunctional allele for the GDNF gene was generated by replacing part of the third exon that encodes the GDNF protein with a cassette expressing the selectable marker neomycin phosphotransferase, as described previously in detail (Pichel et al., 1996). After introducing this construct into embryonic stem cells, six clones were identified with the predicted mutant allele. CD1 or C57BL/6 recipient strains were used to obtain germline transmission of the targeted allele. The mice for this study were bred locally at the Medical University of South Carolina on a C57BL/6J background, weaned, and genotyped as described (Pichel et al., 1996), according to NIH approved protocols. Heterozygous offspring were viable and fertile whereas mice homozygous for the mutant GDNF allele died within 24 h of birth. The mice were housed in groups of 3–4 to a cage and had free access to food and water. They were maintained on a 12-h light:12-h dark cycle at an ambient temperature of 20–22 °C.

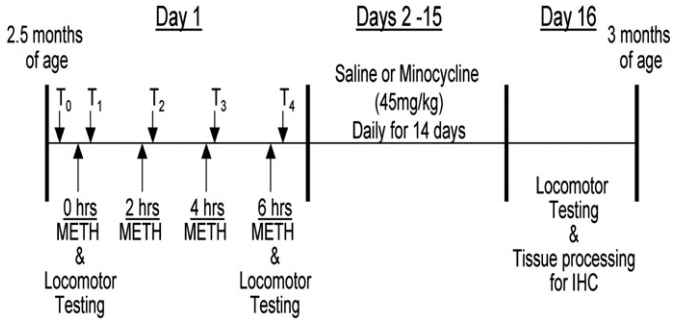

Fig. 1. Experimental design. On day 1, 2.5-month-old GDNF$^{+/-}$ and WT mice were injected 4 times at 2 h intervals with METH (10 mg/kg, i.p.) or saline. Rectal temperatures were recorded 30 min prior to the initiation of injections (T_0) and 20 min following each injection (T_1–T_4). Locomotor activity was recorded for 20 min following the 1st and 4th injections. On days 2–15, starting 24 h after the 4th METH injection, the mice received daily injections of saline or minocycline (45 mg/kg, i.p.). On day 16, locomotor activity was assessed and the mice were perfused and the brains processed for immunohistochemical (IHC) analysis. N=8 per treatment group.

Body temperature measurements

Rectal temperature was measured with a TH-5 Thermalert Monitor Thermometer (Physitemp Instruments, Inc., Clinton, NJ, USA) prior to the first injection and then 20 min after each i.p. METH injection, by holding each mouse at the base of the tail and inserting a probe (RET-3) 2.0 cm past the rectal opening until a constant temperature was maintained for 3 s. Body temperature data at each time point were analyzed with 2 (Genotype)×2 (METH) ANOVAs.

Locomotor activity testing

GDNF$^{+/-}$ and WT mice were tested after the 1st and 4th injections of saline or 10 mg/kg METH according to group assignment, and then again 2 weeks later to evaluate any residual behavioral effects of the METH binge and subsequent minocycline treatment. Locomotor activity (total distance traveled) was assessed in a Digiscan Animal Activity Monitor system for 20 min (Omnitech Electronics Model RXYZCM(8) TAO, Columbus, OH). The details of the apparatus have been described previously (Halberda et al., 1997). Data were collected in one-minute intervals for 20 min at the same time of day (8 am to 12 pm) for each test period. The locomotor activity data for the 1st and 4th injections were analyzed with the 2-way ANOVA described above. The locomotor activity data collected 2 weeks following the METH binge procedure were analyzed with a 2 (Genotype)×2 (METH)×2 (Minocycline) ANOVA.

Immunohistochemistry

After the motor activity tests, mice were anesthetized with halothane and perfused transcardially with saline followed by 4% paraformaldehyde in phosphate buffer (0.1 M, pH 7.4). The brains were removed, post-fixed in 4% paraformaldehyde for 24 h, and then transferred to 30% sucrose in 0.1 M PBS for at least 24 h before sectioning for histochemical analysis. The striatum and midbrain were sectioned on a cryostat (Microm, Zeiss, Thornwood, NY, USA) at 40 µm. Sections through the striatum and SN were processed for free-floating immunohistochemistry using a rabbit polyclonal antibody against TH (1:5000 Pel-Freeze Biologicals, Rogers, AR), or a rat polyclonal antibody against CD45 (1:500 AbD Serotec, Raleigh, NC). Sections through the midbrain were stained with a rabbit polyclonal antibody against phospho-p38 MAPK (1:500 Millipore Biosciences (formerly Chemicon) Temecula, CA). Immunohistochemistry was performed using the avidin-biotin-immunoperoxidase method (Choe and McGinty, 2000). Briefly, after a 5 min pretreatment with 2% Triton-X to allow penetration into the tissue, a subset of sections from each mouse was incubated simultaneously in the primary antisera against TH, CD45, or phospho-p38 MAPK for 24 h at 4 °C. The sections were then rinsed and incubated for 1 h in biotin-conjugated goat anti-rabbit (for TH and phospho-p38 MAPK) or biotin-conjugated rabbit anti-rat (for CD45) IgG, rinsed, and incubated for 1 h in avidin-biotin-peroxidase reagents (Elite Vectastain kit, Vector Labs, Burlingame, CA). The reaction was developed by staining with VIP (Vector Labs, Burlingame, CA) to yield a purple reaction product. Each of the above steps was separated by three 10 min washes in PBS. Sections were mounted on glass slides and coverslipped with DPX. Selected sections immunostained with p38 MAPK-ir were counter-stained with Richardson's (methylene blue/azure II) stain to distinguish glial nuclei from neuronal cell bodies.

Immunohistochemical image analysis

Analysis of striatal TH-ir and SN CD45-ir was performed using the NIH Image program as described previously (Choe and McGinty, 2000). Briefly, background was subtracted and the LUT scale was adjusted using density slicing. This approach captures all labeled

profiles above a threshold density and interactively discriminates them from density values below the threshold. The software then automatically measures the mean optical density and number of pixels per area of the extracted profiles in the selected medial or lateral striatal regions. Two parameters were obtained from this procedure: the *area covered* by the specific profile population (field area), and the *mean density* of the specific profiles. Total immunoreactivity (*integrated density*) was obtained by multiplying the field area times the mean density value. The average number of phosphorylated p38 MAPK-positive cells in the SN was determined using a 1000 μm×200 μm oval encompassing the SN pars compacta (SNpc) starting on a random nigral section approximately −2.92 mm relative to bregma (Paxinos and Franklin, 2001). Measurements were thereafter performed on every 6th section through the SNpc. The hippocampus and mammillary nucleus were used as landmarks in the rostro-caudal plane, and the lateral boundary of the VTA (A10) was used as the medial landmark. Further, the oval excluded the SNpr ventrally, so that the cell body region of the SN was exclusively investigated for phospho-p38 MAPK immunoreactivity. The span of the sectioned tissues exceeded the rostral and caudal extents of the SN, as determined by Nissl staining on an adjacent section series, allowing a systematic random design for the study with a random start within the first sections (see Fig. 3J). Cell counts were conducted with a person blind to the treatment groups. Every 6th section through the SNpc was counted to include four independent sections per animal to generate an average count for each subject. The resulting data were statistically evaluated using a 2 (Genotype)×2 (METH)×2 (Minocycline) ANOVA. Additional analysis included a comparison across groups with a one-way ANOVA followed by Neuman–Keuls multiple comparison tests when a significant *F*-value ($p<0.05$) was obtained.

Results

METH effects on body temperature

The effects of METH on GDNF$^{+/-}$ and WT mice were similar to those previously reported (Boger et al., 2007). Briefly, body temperatures of the four groups did not differ prior to or after the 1st injection whether the mice were injected with METH or saline. However, body temperature was elevated for mice in the METH injected groups mice when assessed after the second ($F_{(1,55)}=28.312$, $p<0.001$), third ($F_{(1,55)}=43.794$, $p<0.001$), and fourth ($F_{(1,55)}=49.376$, $p<0.001$) METH injections. Neither Genotype nor its interaction with the METH binge factor influenced body temperature. Saline-treated mice had stable temperatures across the entire 4 h treatment procedure similar to the basal levels established prior to the injection regimen.

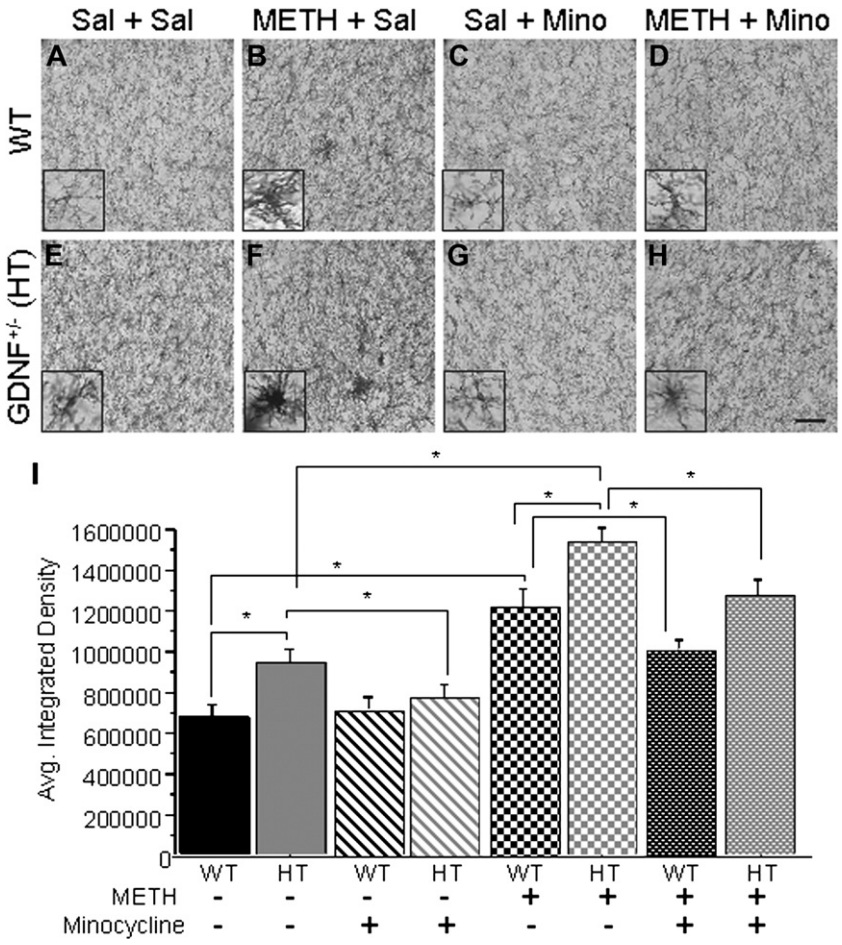

Fig. 2. Minocycline attenuated the METH-induced microglial activation in the SN of GDNF$^{+/-}$ (HT) and WT mice. CD45-ir illustrating activation states of microglia in the SN of WT mice and GDNF$^{+/-}$ mice treated with Sal+Sal (A, E), METH+Sal (B, F), Sal+Mino (C, G), and METH+Mino (D, H). (I) Quantification of the average integrated density of CD45-ir in the SN. Saline-treated GDNF$^{+/-}$ mice had significantly more CD45-ir in the SN than saline-treated WT mice ($p<0.05$). METH induced more CD45-ir in WT mice than saline did ($p<0.05$). Similarly, METH treatment caused a significantly greater increase in CD45-ir in the SN of GDNF$^{+/-}$ mice 2 weeks after injection than saline did. This increase was greater in GDNF$^{+/-}$ mice than in METH-treated WT mice ($p<0.05$). Minocycline treatment reduced CD45-ir in saline-treated GDNF$^{+/-}$ mice to levels comparable to saline-treated WT mice. Also, minocycline attenuated the CD45-ir in mice treated previously with METH, although not to levels comparable to saline-treated mice. Sal=saline, METH=methamphetamine, Mino=minocycline. $N=8$ per group (*$p=0.05$). Scale bar=100 μM. Inset pictures are 60× magnification of resting, active, and reactive microglia.

Locomotor activity

As previously described (Boger et al., 2007), motor activity during the first assessment was greater for METH- than saline-treated mice ($F_{(1,55)}$=21.343, p<0.0001) with no effect of Genotype or its interaction with drug. After the fourth injection, motor activity of METH-treated mice was lower than that of saline-treated controls ($F_{(1,55)}$=7.807, p<0.0001), again with no influence of Genotype or its interaction with drug. When tested after the 14-day minocycline regimen, motor activity did not vary according to any of the three factors or across any of the eight treatment groups (data not shown).

Substantia nigra microglial activation

The microglial response in the SN to the toxic METH binge is illustrated in Fig. 2. Microglia were stained with a CD45 antibody that detects cluster differentiation marker 45. Resting state microglia are characterized by a smaller cell body with long, thin processes (see Fig. 2A inset), whereas reactive microglia are characterized by increased cell body volume, short, thick processes, and increased intensity of staining for cell surface markers, such as CD45 (see Figs. 2B and F insets; Lavoie et al., 2004). Because CD45 is expressed by both resting and activated microglia, qualitative assessment of the morphological appearance of microglia supplemented density measurements.

The integrated density data (Fig. 2I) indicate higher average CD45-ir integrated density values for GDNF$^{+/-}$ than WT mice (Genotype: $F_{(1,47)}$=5.566, p<0.05) and for METH- compared to saline-treated mice (METH: $F_{(1,47)}$=76.205, p<0.0001) with no interaction of the main factors. Additional analysis with one-way ANOVAs established group differences ($F_{(7,47)}$= 13.091, p<0.001). Neuman–Keuls analyses indicated greater density of CD45-ir in the SN of GDNF$^{+/-}$ than in WT mice treated with saline (p<0.05; Figs. 2A, E, I), as previously reported (Boger et al., 2007). In addition, CD45-ir was elevated in SN of both WT and GDNF$^{+/-}$ mice subjected to the METH binge compared to their respective saline controls (p<0.05; Figs. 2A, B, E, F, I). Although METH treatment elevated CD45-ir in the SN of WT and GDNF$^{+/-}$ mice, the additive contributions of genotype and METH resulted in the highest CD45-ir for GDNF$^{+/-}$ mice subjected to the METH binge (p<0.05; Figs. 2B, E, F, I).

The two-week minocycline regimen lowered CD45-ir ($F_{(1,47)}$=5.981, p<0.05) with no interaction of the Minocycline factor with either Genotype or METH treatment factors. Neuman–Keuls tests following the one-way ANOVA established that minocycline reduced the elevated CD45-ir in the SN of saline-treated GDNF$^{+/-}$ mice to levels no different from the saline-treated WT mice (p<0.05). This minocycline-induced reduction in CD45 immunoreactivity is complemented by the similar morphological appearance of the microglia in minocycline-treated mice (Fig. 2G inset) and saline-treated WT mice (Fig. 2A inset). Similarly, METH-induced microglial activation was reduced in both WT and GDNF$^{+/-}$ mice following treatment with minocycline (p<0.05, Figs. 2D, H, I). However, the CD45 staining levels in METH-treated mice were not reduced to those of saline-treated mice, regardless of genotype.

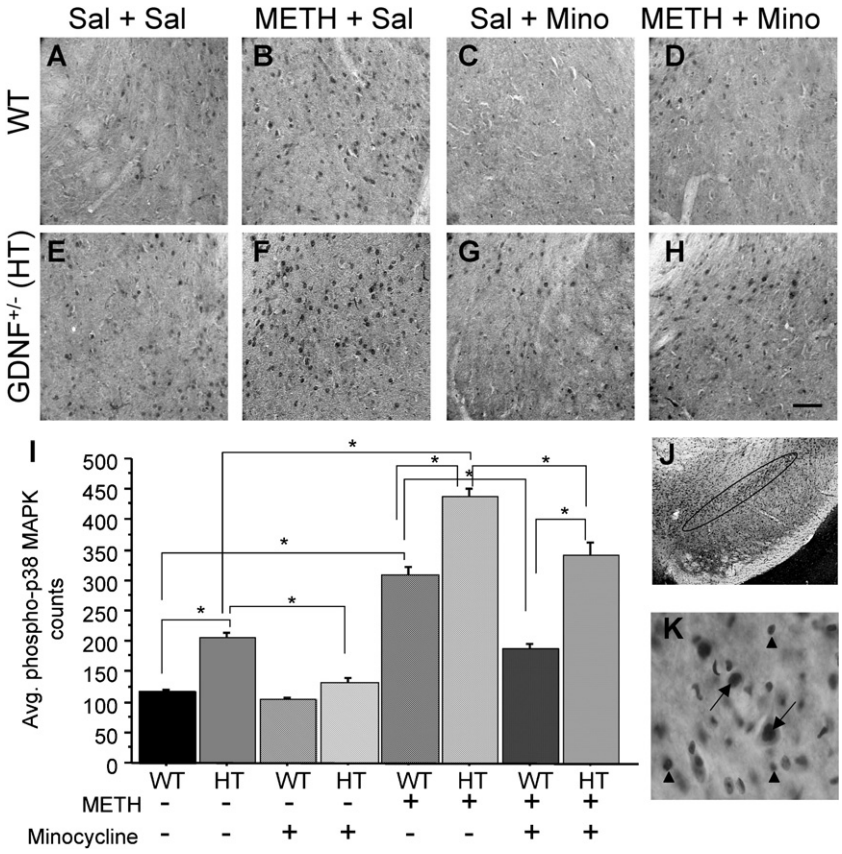

Fig. 3. Phosphorylated p38 MAPK in the SN is decreased after minocycline treatment. Photomicrograph of p38 MAPK phosphorylation in the midbrain of WT and GDNF$^{+/-}$ mice treated with Sal+Sal (A, E), METH+Sal (B, F), Sal+Mino (C, G), and METH+Mino (D, H). (I) Quantitation of the average number of phosphorylated p38 MAPK cells in the SN. (J) Photomicrograph of Nissl stained section outlining the SNpc used for phospho-p38 MAPK counts. (K) 60× oil magnification demonstrating localization of phospho-p38 MAPK in the nucleus of neurons (arrows). No localization of phospho-p38 MAPK was observed in glial cells (arrow heads). Saline-treated GDNF$^{+/-}$ mice demonstrated more phospho-p38 MAPK than saline-treated WT mice (p<0.05). METH treatment increased the number of phosphorylated p38 MAPK-positive cells, with the greatest increase seen in METH-treated GDNF$^{+/-}$ mice (C, G; p<0.05). Minocycline decreased the number of phospho-p38 MAPK-positive cells in the SN of saline-treated GDNF$^{+/-}$ mice (p<0.05). Furthermore, minocycline reduced the METH-induced phosphorylation of p38 MAPK-ir (p<0.05). Sal=saline, METH=methamphetamine, Mino=minocycline. N=8 per group (*p=0.05). Scale bar=100 μM.

Substantia nigra p38 MAPK phosphorylation

Because of the low constitutive expression of phospho-p38 MAPK and its confinement to discrete somal profiles when induced, cell counting was used to detect differences among groups. As can be appreciated from Fig. 3K, phospho-p38 MAPK-ir was localized to the nucleus of neurons, with no indication of immunolabeling in glial cells. A significant Genotype×METH interaction ($F_{(1,47)}=28.380$, $p<0.0001$) was revealed for phospho-p38 MAPK cell counts in the SN (Fig. 3). Further analysis by one-way ANOVA demonstrated group differences ($F_{(7,47)}=123.400$, $p<0.001$). Neuman–Keuls analyses indicated that saline-treated GDNF$^{+/-}$ mice had a greater number of phospho-p38 MAPK stained cell bodies than saline-treated WT mice ($p<0.05$, Figs. 3A, E, I). 2 weeks after a toxic binge of METH, phospho-p38 MAPK counts were increased in the SN of WT and GDNF$^{+/-}$ mice ($p<0.05$), with the highest number observed in METH-treated GDNF$^{+/-}$ mice (Figs. 3B, F, I).

The 14-day regimen of minocycline resulted in a significant Genotype×METH×Minocycline interaction ($F_{(1,47)}=8.027$, $p<0.01$). Neuman–Keuls analysis after the one-way ANOVA demonstrated that minocycline attenuated the number of phospho-p38 MAPK cells in saline-treated GDNF$^{+/-}$ mice ($p<0.05$; Figs. 3C, G, I). Similarly, the METH-induced increase of p38 MAPK immunoreactivity was decreased in mice treated with minocycline, regardless of genotype, although the % decrease was greater in WT mice ($p<0.05$, Figs. 4D, H, I). There was a positive correlation ($r=0.972$; $p<0.001$) between SN CD45-ir and SN phospho-p38 MAPK-positive cells in saline-treated WT mice that underwent the minocycline regimen, suggesting that there is an integral relationship between phosphorylation of p38 MAPK and microglial activation. Saline-treated GDNF$^{+/-}$ mice also had a positive correlation between SN CD45-ir and SN phospho-p38 MAPK counts after a 14-day regimen of minocycline ($r=0.983$; $p<0.001$). No other group displayed a correlation between these two immunohistochemical measurements.

Tyrosine hydroxylase immunohistochemistry

In the lateral region of the striatum, there were significant Genotype ($F_{(1,47)}=6.665$, $p<0.05$) and METH treatment ($F_{(1,47)}=130.317$, $p<0.05$) effects, with no effect of minocycline treatment or interactions of the main factors. In addition, group differences existed as demonstrated by one-way ANOVA analysis ($F_{(7,47)}=19.095$, $p<0.001$). Neuman–Keuls analysis revealed that TH-ir in the lateral striatum was similar in the saline+saline and the saline+minocycline-treated groups, regardless of genotype (Figs. 4A, B, E, F, I-left). METH treatment caused a greater reduction of TH-ir in the lateral striatum of GDNF$^{+/-}$ (93%) than in WT (69%) mice 2 weeks after injections ($p<0.05$; Figs. 4C, G and I-left). The 14-day regimen of minocycline

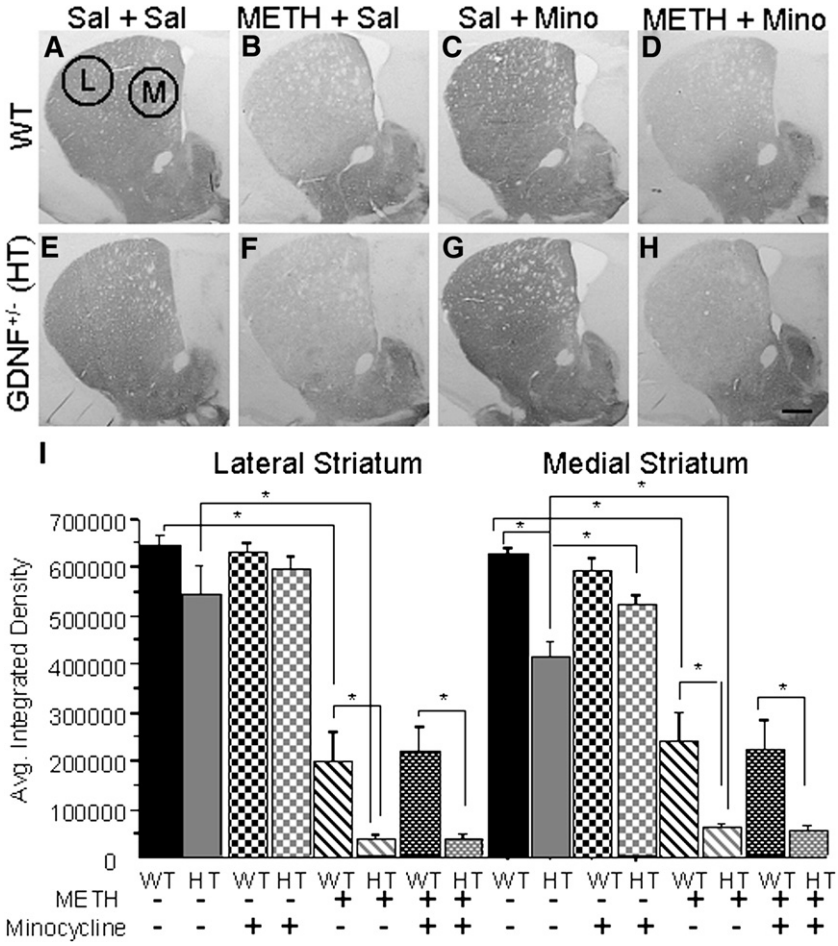

Fig. 4. METH-induced striatal TH depletion is unaffected by minocycline treatment. Striatal TH-ir images from WT and GDNF$^{+/-}$ mice treated with Sal+Sal (A, E), METH+Sal (B, F), Sal+Mino (C, G), and METH+Mino (D, H). Medial (M) and lateral (L) striatal selection areas are illustrated. (I) Quantification of the average integrated density of striatal TH-ir between the different treatment groups. No differences existed in the lateral region of the striatum between the GDNF$^{+/-}$ and WT mice treated with saline. In the medial region, the GDNF$^{+/-}$ mice displayed less TH-ir. 2 weeks after the METH binge, METH-induced a similar TH-ir depletion in the lateral striatum of GDNF$^{+/-}$ and WT mice when compared to saline treated mice ($p<0.05$) and a significantly greater depletion in the medial striatum of GDNF$^{+/-}$ than WT mice ($p<0.05$). Minocycline treatment increased the TH-ir in the medial striatum of saline-treated GDNF$^{+/-}$ mice compared to non-minocycline treated GDNF$^{+/-}$ mice ($p<0.05$). However, minocycline did not have any effect on TH-ir in METH-treated mice, regardless of genotype. Sal=saline, METH=methamphetamine, Mino=minocycline. $N=8$ per group (*$p=0.05$). Scale bar=0.5 mm.

had no effect on METH-induced reductions of TH-ir in the lateral striatum.

Similarly, in the medial region of the striatum, significant Genotype ($F_{(1,47)}=5.734$, $p<0.05$) and METH treatment ($F_{(1,47)}=111.455$, $p<0.05$) effects existed with no effect of minocycline treatment or interactions of the main factors. Group differences existed in medial striatum TH-ir as demonstrated by one-way ANOVA analysis ($F_{(7,47)}=16.607$, $p<0.001$). Neuman–Keuls analysis indicated that saline+saline-treated GDNF$^{+/-}$ mice had lower TH-ir staining compared to age-matched WT mice ($p<0.05$; Figs. 4A, E, I-right). In contrast, saline-treated GDNF$^{+/-}$ mice treated with minocycline for 14 days displayed an increase in TH-ir in the medial striatum as compared to saline+saline-treated GDNF$^{+/-}$ mice ($p<0.05$; Figs. 4E, G, I). No effect of minocycline treatment was evident in WT mice (saline+mino group). Furthermore, METH treatment produced a significantly greater decrease in TH-ir in the medial striatum of GDNF$^{+/-}$ (89%) than in WT (55%) mice ($p<0.05$; Figs. 4B, F and I-right). Minocycline treatment had no effect on the METH-induced decrease in TH-ir, regardless of genotype (Figs. 4D, H, I). These data indicate that minocycline was able to increase striatal TH-ir in mice with a partial depletion of GDNF but was not able to rescue the METH-induced striatal DAergic depletion, regardless of genotype.

Discussion

Confirming our previous report (Boger et al., 2007), 3 month-old mice with a genetic GDNF deficiency had greater microglial activation in SN and less TH-ir than WT controls. Further, a minocycline treatment paradigm, with demonstrated efficacy in animal models of neurotoxicity, attenuated the SN microglial activation and the phospho-p38 MAPK response in the saline-treated GDNF$^{+/-}$ mice and in mice of both genotypes exposed to the METH binge. Minocycline also attenuated the lower TH-ir levels in the medial striatum that characterize GDNF$^{+/-}$ vs. WT mice. Despite reducing inflammation, minocycline did not prevent the METH-induced TH-ir loss in the striatum in mice of both genotypes. The ability of minocycline to attenuate the TH-ir reduction in mice with a genetic reduction of GDNF, but not the METH-induced TH-ir reduction, suggests different mechanisms of TH-ir regulation and depletion.

Substantia nigra microglial activation

Microglial activation is associated with various types of brain injury in humans (Kato et al., 2000), with neurotoxic chemical damage in animal models of various diseases (Jorgensen et al., 1993; Scali et al., 1999; Fiedorowicz et al., 2001) and with the DAergic neurodegeneration characterizing PD and animal models of PD (Francis et al., 1995; Czlonkowska et al., 1996; Langston et al., 1999). In the present study, microglial activation was observed in the SN, but not the striatum, of 3-month-old GDNF$^{+/-}$, but not WT mice, confirming our previous findings (Boger et al., 2007). Our previous work established that in spite of the microglial activation in the young adult GDNF$^{+/-}$ mice, loss of TH-positive neurons in SN is not evident until mid-life (12 months of age; Boger et al., 2006, 2007). The delayed loss suggests that chronic SN microglial activation might weaken the integrity of DAergic neurons, leading to cell death later in life.

The minocycline treatment in our study decreased the density of CD45-ir and phospho-p38 MAPK cell counts and attenuated the reduction in striatal TH-ir in GDNF$^{+/-}$ mice to the level obtained for WT mice. The ability of minocycline to attenuate differences in these three parameters of nigrostriatal integrity in GDNF$^{+/-}$ and WT mice suggests that chronic inflammation contributes to the DA neuronal damage in the GDNF$^{+/-}$ mice. Minocycline attenuated the microglial activation in METH binge-treated mice of both genotypes; however, not to the levels of saline-treated mice. The finding that the anti-inflammatory action of minocycline did not protect DAergic neurons from METH-induced damage is consistent with a report that minocycline reduced the inflammatory markers, interleukin-6, F4/80, and interleukin-1α, in the striatum of MPTP-treated and METH-treated mice but did not prevent MPTP-induced toxicity unless TNFα 1 and 2 receptors were deleted (Sriram et al., 2006). Thus, attenuating microglial activation is not sufficient to protect against METH-induced striatal DAergic damage nor does it eliminate the exacerbated DAergic toxicity METH produces in GDNF$^{+/-}$ mice. Future experiments to assess the contribution of TNFα and/or other pro-inflammatory cytokines to METH-induced striatal damage in GDNF$^{+/-}$ mice are necessary to establish the mechanism underlying the interaction between GDNF depletion and METH-induced damage.

The increase in phosphorylated p38 MAPK in the SN of naïve young adult GDNF$^{+/-}$ compared to WT mice and the further increase produced by the METH binge in combination with increased microglial activation in these mice suggest that the p38 MAPK pathway may be activated in response to cell stressors such as, in this case, genetic and neurotoxin-induced neuroinflammation. The blockade of p38 MAPK can therefore be expected to benefit neuronal populations affected by microglial activation and inflammation by activating transcription factors that regulate the induction of cell stress mechanisms, such as inflammatory genes (Bhat et al., 1998). In vitro studies indicate that minocycline exerts protective effects in different ways, including the reduction of p38 MAPK phosphorylation (Du et al., 2001; Wu et al., 2002; Hunter et al., 2004). Because minocycline reduced phospho-p38 MAPK staining in GDNF$^{+/-}$ vs. WT mice, as well as mice of both genotypes exposed to a toxic binge of METH without affecting the TH-ir reduction, phospho-p38 MAPK appears not to contribute to METH-induced TH-ir depletion.

Tyrosine hydroxylase immunohistochemistry

Minocycline treatment prevented the reduced levels of striatal TH-ir observed in young GDNF$^{+/-}$ mice relative to WT control mice, suggesting that SN inflammation contributes to the reduced DAergic innervation of striatum in these mice. This restorative effect of minocycline in GDNF$^{+/-}$ mice could be due to the reversal of microglia-exacerbated injury to astrocytes as reported by Yenari et al. (2006). In that study, the addition of microglia to endothelial cell/astrocyte co-cultures increased cell death; however, minocycline prevented the microglial-induced increased injury. Future studies to determine if minocycline increases GDNF will be necessary to establish whether or not GDNF provides a biological substrate for minocycline-mediated neuroprotection.

In contrast to its restorative effects in saline-treated GDNF$^{+/-}$ mice, minocycline did not restore the striatal TH loss associated with the toxic METH binge. The absence of a minocycline effect on METH-induced DAergic damage suggests that inflammation is not a necessary condition for METH toxicity. An alternative possibility is that METH stimulates spectrin proteolysis, which is mediated via calpain activation in a time-dependent manner within the striatum (Staszewski and Yamamoto, 2006). Interestingly, proteolysis of spectrin, a cytoskeletal protein contributing to neuronal integrity, has been proposed as an important component of neuronal death (Lowy et al., 1995). It should be noted, however, that minocycline has been reported to be protective in experimental conditions which promote caspase, rather than calpain, induction (Bantubungi et al., 2005). Minocycline was also not protective in a Huntington's disease model (3-nitropropionic) in which striatal neurotoxic damage was associated with increased calpain (not caspase) activation (Bantubungi et al., 2005). Since dose-dependent differences in minocycline efficacy have been reported (Yrjanheikki et al., 1999; Ahuja et al., 2007), it might be argued that the particular dosing paradigm used in our study prevented its efficacy against METH-induced DAergic toxicity. However, the minocycline dosing paradigm effectively

attenuated METH-induced phospho-p38 MAPK and CD45-ir in the present study making this an unlikely interpretation. Finally, there is evidence that METH damages DA neuronal terminals by generating nitric oxide and reactive oxygen species (for a review see Imam et al., 2000). In fact, a radical scavenger, edaravone, reportedly blocks METH-induced DA neuron toxicity without decreasing METH-induced inflammation (Kawasaki et al., 2006), making radical oxygen species formation a likely mechanism underlying the METH-induced damage in this study.

In conclusion, the present study demonstrated that minocycline suppressed microglial activation and decreased the phosphorylated state of p38 MAPK in the SN of GDNF$^{+/-}$ mice and mice administered a toxic regimen of METH. Additionally, minocycline partially rescued DAergic damage associated with a genetic reduction of GDNF; however, minocycline did not protect the DAergic terminals from METH-induced toxicity. Thus, while TH expression in GDNF$^{+/-}$ mice was enhanced by minocycline, the toxic effects of METH on DA neurons were not reversed and, therefore, must depend on other biological mechanisms, such as mitochondrial dysfunction, oxidative stress, or glutamate excitotoxicity.

Acknowledgments

We thank Alfred Moore and Joe Vallone for technical assistance. This work was supported by PO1 AG023630 and by C06 RR015455 from the Extramural Research Facilities Program of the National Center for Research Resources.

References

Ahuja, M., Bishnoi, M., Chopra, K., 2007. Protective effect of minocycline, a semi-synthetic second-generation tetracycline against 3-nitropropionic acid (3-NP)-induced neurotoxicity. Toxicology 244, 111–122.

Bantubungi, K., Jacquard, C., Greco, A., Pintor, A., Chtarto, A., Tai, K., Galas, M.C., Tenenbaum, L., Deglon, N., Popoli, P., Minghetti, L., Brouillet, E., Brotchi, J., Levivier, M., Schiffmann, S.N., Blum, D., 2005. Minocycline in phenotypic models of Huntington's disease. Neurobiol. Dis. 18, 206–217.

Bhat, N.R., Zhang, P., Lee, J.C., Hogen, H.L., 1998. Extracellular signal-regulated kinase and p38 subgroups of MAP kinases regulate inducible nitric oxide synthase and tumor necrosis factor gene expression in endotoxin stimulated primary glial cultures. J. Neurosci. 18, 1633–1641.

Boger, H.A., Middaugh, L.D., Huang, P., Zaman, V., Smith, A.C., Hoffer, B.J., Tomac, A.C., Granholm, A.-Ch., 2006. A partial GDNF depletion leads to earlier age-related deterioration of motor function and tyrosine hydroxylase expression in the substantia nigra. Exp. Neurol. 202, 336–347.

Boger, H.A., Middaugh, L.D., Patrick, K.S., Ramamoorthy, S., Denehy, E.D., Zhu, H., Pacchioni, A.M., Granholm, A.-Ch., McGinty, J.F., 2007. Longterm consequences of methamphetamine exposure in young adults are exacerbated in glial cell line-derived neurotrophic factor heterozygous mice. J. Neurosci. 27, 8816–8825.

Blum, D., Chtarto, A., Tenenbaum, L., Brotchi, J., Levivier, M., 2004. Clinical potential of minocycline for neurodegenerative disorders. Neurobiol. Dis. 17, 359–366.

Chen, C.C., Wang, J.K., 1999. p38 but not p44/42 mitogen-activated protein kinase is required for nitric oxide synthase induction mediated by lipopolysaccharide in RAW 264.7 macrophages. Mol. Pharmacol. 55, 481–488.

Chen, M., Ona, V.O., Li, M., Ferrant, R.J., Fink, K.B., Zhu, S., Bian, J., Guo, L., Farrell, L.A., Hersch, S.M., Hobbs, W., Vonsattel, J.P., Cha, J.H., Friendlander, R.M., 2000. Minocycline inhibits caspase-1 and caspase-3 expression and delays mortality in a transgenic mouse model of Huntington disease. Nat. Med. 6, 797–801.

Choe, E.S., McGinty, J.F., 2000. NMDA receptors and p38MAP kinase are required for cAMP-dependent CREB and Elk-1 phosphorylation in the striatum of rats. Neuroscience 101, 607–617.

Czlonkowska, A., Kohutnicka, M., Kurkowska-Jastrzebska, I., Czlonkowski, A., 1996. Microglial reaction in MPTP (1-methyl-4-phenyl-1,2,3,6-tetrahydropyridine) induced Parkinson's disease mice model. Neurodegeneration 5, 137–143.

Diguet, E., Fernagut, P.O., Wei, X., Du, Y., Rouland, R., Gross, C., Bezard, E., Tison, F., 2004. Deleterious effects of minocycline in animal models of Parkinson's disease and Huntington's disease. Eur. J. Neurosci. 19, 3266–3276.

Du, Y., Ma, Z., Lin, S., Dodel, R.C., Gao, F., Bales, K.R., Triarhou, L.C., Chernet, E., Perry, K.W., Nelson, D.L.G., Luecke, S., Phebus, L.A., Bymaster, F.P., Paul, S., 2001. Minocycline prevents nigrostriatal dopaminergic neurodegeneration in the MPTP model of Parkinson's disease. Proc. Natl. Acad. Sci. U. S. A. 98, 14669–14674.

Fiedorowicz, A., Figiel, I., Kaminska, B., Zaremba, M., Wilk, S., Oderfeld-Nowak, B., 2001. Dentate granule neuron apoptosis and glia activation in murine hippocampus induced by trimethyltin exposure. Brain Res. 912, 116–127.

Francis, J.W., Von Visger, J., Markelonis, G.J., Oh, T.H., 1995. Neuroglial responses to the dopaminergic neurotoxicant 1-methyl-4-phenyl-1,2,3,6-tetrahydropyridine in mouse striatum. Neurotoxicol. Teratol. 17, 7–12.

Glicksman, M.A., Chiu, A.Y., Dionne, C.A., Harty, M., Kaneko, M., Murakata, C., Oppenheim, R.W., Prevette, D., Sengelaub, D.R., Vaught, J.L., Neff, N.T., 1998. CEP-1347/KT7515 prevents motor neuronal programmed cell death and injury-induced dedifferentiation in vivo. J. Neurobiol. 35, 361–370.

Gordon, P.H., Moore, D.H., Miller, R.G., Florence, J.M., Verheijde, J.L., Doorish, C., Hilton, J.F., Spitalny, G.M., MacAurthur, R.B., Mitsumoto, H., Neville, H.E., Boylan, K., Mozaffar, T., Belsh, J.M., Ravits, J., Bedlack, R.S., Graves, M.C., McCluskey, L.F., Barohn, R.J., Tandan, R., 2007. Efficacy of minocycline in patients with amyotrophic lateral sclerosis: a phase III randomised trial. Lancet Neurol. 6, 1045–1053.

Halberda, J.P., Middaugh, L.D., Gard, B.E., Jackson, B.P., 1997. DAD1- and DAD2-like agonist effects on motor activity of C57 mice: differences compared to rats. Synapse 26, 81–92.

Hebert, M.A., O'Callaghan, J.P., 2000. Protein phosphorylation cascades associated with methamphetamine-induced glial activation. Ann. N. Y. Acad. Sci. 914, 238–262.

Hendricks, B.S., Hua, F., Chabot, J.R., 2008. Analysis of mechanistic pathway models in drug discovery: p38 pathway. Biotechnol. Prog. 24, 96–109.

Hunter, C.L., Quintero, E.M., Gilstrap, L., Bhat, N.R., Granholm, A.-Ch., 2004. Minocycline protects basal forebrain cholinergic neurons from mu p75-saporin immunotoxic lesioning. Eur. J. Neurosci. 19, 3305–3316.

Imam, S.Z., Islam, F., Itzhak, Y., Slikker Jr., W., Ali, S., 2000. Prevention of dopaminergic neurotoxicity by targeting nitric oxide and peroxynitrite: implication for the prevention of methamphetamine-induced neurotoxic damage. Ann. N. Y. Acad. Sci. 914, 157–171.

Jorgensen, M.B., Finsen, B.R., Jensen, M.B., Castellano, B., Diemer, N.H., Zimmer, J., 1993. Microglial and astroglial reactions to ischemic and kainic acid-induced lesions of the adult rat hippocampus. Exp. Neurol. 120, 70–88.

Kato, H., Tanaka, S., Oikawa, T., Koike, T., Takahashi, A., Itovama, Y., 2000. Expression of microglial response factor-1 in microglia and macrophages following cerebral ischemia in the rat. Brain Res. 882, 206–211.

Kawasaki, H., Morooka, T., Shimohama, S., Kimura, J., Hirano, T., Gotoh, Y., Nishida, E., 1997. Activation and involvement of p38 mitogen-activated protein kinase in glutamate-induced apoptosis in rat cerebellar granule cells. J. Biol. Chem. 272, 18518–18521.

Kawasaki, T., Ishihara, K., Yukio, A., Nakamura, S., Itoh, S., Baba, A., Matsuda, T., 2006. Protective effect of the radical scavenger edaravone against methamphetamine-induced dopaminergic neurotoxicity in mouse striatum. Eur. J. Pharmacol. 542, 92–99.

Kriz, J., Nguyen, M.D., Julien, J.P., 2002. Minocycline slows disease progression in a mouse model of amyotrophic lateral sclerosis. Neurobiol. Dis. 10, 268–278.

Langston, J.W., Forno, L.S., Tetrud, J., Reeves, A.G., Kaplan, J.A., Karluk, D., 1999. Evidence of active nerve cell degeneration in the substantia nigra of humans years after 1-methyl-4-phenyl-1,2,3,6-tetrahydropyridine exposure. Ann. Neurol. 46, 598–605.

Lavoie, M.J., Card, J.P., Hastings, T.G., 2004. Microglial activation preceded dopamine terminal pathology in methamphetamine-induced neurotoxicity. Exp. Neurol. 187, 47–57.

Lee, J.C., Laydon, J.T., McDonnel, P.C., Gallagher, T.F., Kumar, S., Green, D., McNulty, D., Blumenthal, M.J., Heys, J.R., Landyatter, S.W., Strickler, J.E., McLaughlin, M.M., Siemens, I.R., Fisher, S.M., Livi, G.P., White, J.R., Adams, J.L., Young, P.R., 1994. A protein kinase involved in the regulation of inflammatory cytokine biosynthesis. Nature 372, 739–746.

LeWitt, P.A., Taylor, D.C., 2008. Protection against Parkinson's disease: clinical experience. Neurotherapeutics 5, 210–225.

Lowy, M.T., Wittenberg, L., Yamamoto, B.K., 1995. Effect of acute stress on hippocampal glutamate levels and spectrin proteolysis in young and aged rats. J. Neurochem. 65, 268–274.

Paxinos, G., Franklin, K.B.J., 2001. The Mouse Brain in Stereotaxic Coordinates: Deluxe Edition of the Atlas, Second ed. Academic Press, San Diego, CA, USA.

Pichel, J.G., Shen, L., Sheng, H.Z., Granholm, A.-Ch., Drago, J., Grinberg, A., Lee, E.J., Huang, S.P., Saarma, M., Hoffer, B.J., Sariola, H., Westphal, H., 1996. Defects in enteric innervation and kidney development in mice lacking GDNF. Nature 382, 73–76.

Quintero, E.M., Willis, L., Singleton, R., Harris, N., Huang, P., Bhat, N.R., Granholm, A.-Ch., 2006. Behavioral and morphological effects of minocycline in the 6-hydroxydopamine rat model of Parkinson's disease. Brain Res. 1093, 198–207.

Scali, C., Prosperi, C., Giovannelli, L., Bianchi, L., Pepeu, G., Casamenti, F., 1999. Beta(1–40) amyloid peptide injection into the nucleus basalis of rats induces microglia reaction and enhances cortical gamma-aminobutyric acid release in vivo. Brain Res. 831, 319–321.

Sheng, P., Cerruti, C., Cadet, J.L., 1994. Methamphetamine (METH) causes reactive gliosis in vitro: attenuation by the ADP-ribosylation (ADPR) inhibitor, benzamide. Life Sci. 55, PL51–PL54.

Sriram, K., Miller, D.B., O'Callaghan, J.P., 2006. Minocycline attenuates microglial activation but fails to mitigate striatal dopaminergic neurotoxicity: role of tumor necrosis factor-alpha. J. Neurochem. 96, 706–718.

Staszewski, R.D., Yamamoto, B.K., 2006. Methamphetamine-induced spectrin proteolysis in the rat striatum. J. Neurochem. 96, 1267–1276.

Thomas, D.M., Dowgiert, J., Geddes, T.J., Francescutti-Verbeem, D., Liu, X., Kuhn, D.M., 2004a. Microglial activation is a pharmacologically specific marker for the neurotoxic amphetamines. Neurosci. Lett. 367, 349–354.

Thomas, D.M., Walker, P.D., Benjamins, J.A., Geddes, T.J., Kuhn, D.M., 2004b. Methamphetamine neurotoxicity in dopamine nerve endings of the striatum is associated with microglial activation. J. Pharmacol. Exp. Ther. 311, 1–7.

Tikka, T., Koistinaho, J., 2001a. Minocycline provides neuroprotection against NMDA neurotoxicity by inhibiting microglia. J. Immunol. 166, 7527–7533.

Tikka, T., Fiebich, B., Goldsteins, G., Keinanen, R., Koistinaho, J., 2001b. Minocycline, a tetracycline derivative, is neuroprotective against excitotoxicity by inhibiting activation and proliferation of microglia. J. Neurosci. 21, 2580–2588.

Tsuji, M., Wilson, M.A., Lange, M.S., Johnston, M.V., 2004. Minocycline worsens hypoxic-ischemic brain injury in a neonatal mouse model. Exp. Neurol. 189, 58–65.

Wang, X., Zhu, S., Drozda, M., Zhang, W., Stavrovskava, I.G., Cattaneo, E., Ferrante, R.J., Kristal, B.S., Friedlander, R.M., 2003. Minocycline inhibits caspase-independent and -dependent mitochondrial cell death pathways in models of Huntington's disease. Proc. Natl. Acad. Sci. U. S. A. 100, 10483–10487.

Wang, J., Wei, Q., Wang, C.Y., Hill, W.D., Hess, D.C., Dong, Z., 2004. Minocycline up-regulates Bcl-2 and protects against cell death in the mitochondria. J. Biol. Chem. 279, 19948–19954.

Wu, D.C., Jackson-Lewis, V., Vila, M., Tieu, K., Teismann, P., Vadseth, C., Choi, D.-K., Ischiropoulos, H., Przedborski, S., 2002. Blockade of microglial activation is neuroprotective in the 1-methyl-4-phenyl-1,2,3,6-tetrahydropyridine mouse model of Parkinson's disease. J. Neurosci. 22, 1763–1771.

Yang, L., Sugama, S., Chirichigno, J.W., Gregorio, J., Lorenzl, S., Shin, D.H., Browne, S.E., Shimizu, Y., Joh, T.H., Beal, M.F., Albers, D.S., 2003. Minocycline enhances MPTP toxicity to dopaminergic neurons. J. Neurosci. Res. 74, 278–285.

Yenari, M.A., Xu, L., Tang, X.N., Oiao, Y., Giffard, R.G., 2006. Microglia potentiate damage to blood–brain barrier constituents: improvement by minocycline in vivo and in vitro. Stroke 37, 1087–1093.

Yrjanheikki, J., Keinanen, R., Pellikka, M., Hokfelt, T., Koistinaho, J., 1998. Tetracyclines inhibit microglial activation and are neuroprotective in global brain ischemia. Proc. Natl. Acad. Sci. U. S. A. 95, 15769–15774.

Yrjanheikki, J., Tikka, T., Keinanen, R., Goldsteins, G., Chan, P.H., Koistinaho, J., 1999. A tetracycline derivative, minocycline, reduces inflammation and protects against focal cerebral ischemia with a wide therapeutic window. Proc. Natl. Acad. Sci. U. S. A. 96, 13496–13500.

Zawada, W.M., Meintzer, M.K., Rao, P., Marotti, J., Wang, X., Esplen, J.E., Clarkson, E.D., Freed, C.R., Heidenreich, K.A., 2001. Inhibitors of p38 MAP kinase increase the survival of transplanted dopamine neurons. Brain Res. 891, 185–196.

Zhu, S., Stravroskaya, I.G., Drozda, M., Kim, B.Y., Ona, V., Li, M., Sarang, S., Liu, A.S., Hartley, D.M., Wu, D.C., Gullans, S., Ferrante, R.J., Przedborski, S., Kristal, B.S., Friedlander, R.M., 2002. Minocycline inhibits cytochrome c release and delays progression of amyotrophic lateral sclerosis in mice. Nature 417, 74–78.